Scanning Electron Microscopy

Volume 1986 | Number 2 Article 41

4-29-1986

The Determination of Wet Weight Concentrations of Elements in Freeze-Dried Cryosections from Biological Cells

Karl Zierold
Max-Planck-Institut für Systemphysiologie

SCANNING ELECTRON MICROSCOPY/1986/II (Pages 713-724)
SEM Inc., AMF O'Hare (Chicago), IL 60666-0507 USA

0586-5581/86$1.00+05

THE DETERMINATION OF WET WEIGHT CONCENTRATIONS OF ELEMENTS IN FREEZE-DRIED CRYOSECTIONS FROM BIOLOGICAL CELLS

Karl Zierold

Max-Planck-Institut für Systemphysiologie
Rheinlanddamm 201
D-4600 Dortmund, FRG
Phone No. (0231) 12 06 455

(Received for publication February 11, 1986: revised paper received April 29, 1986)

Abstract

Energy dispersive X-ray microanalysis in STEM (scanning transmission electron microscope) of freeze-dried cryosections from biological cells provides information on the subcellular element distribution in terms of dry weight concentration. The local dry weight content in the range of 5-50%, respectively the local water content within 50 to 95%, in different subcellular compartments can be determined by measuring the darkfield intensity by means of an annular detector in STEM. Calibration is done by measuring the darkfield intensity of similarly prepared cryosections from dextran-water-solutions in varying concentration. Thus, by combining the X-ray microanalytical data evaluated by the continuum method with the STEM darkfield values, wet weight concentrations of elements in subcellular compartments are obtained. The method was applied to fibroblast cells in suspension. The reliability of this method is compared with other techniques to measure mass and intracellular water by electron microscope methods.

KEY WORDS: biological X-ray microanalysis, cryosection, darkfield electron microscopy, diffusible ions, dry weight concentration, freeze-drying, intracellular water, STEM, water distribution, wet weight concentration

Introduction

The preparation of freeze-dried cryosections for electron probe microanalysis in order to determine the distribution of elements in different compartments of biological cells has been described by several authors (see e.g., Somlyo et al., 1977; Somlyo and Shuman, 1982; Hall and Gupta, 1983; Hagler and Buja, 1984; Rick et al., 1982; Roomans et al., 1982; Wendt-Gallitelli and Wolburg, 1984; Zierold, 1982, 1984a, 1986). The method consists essentially of the following procedure: 1. Cryofixation of the biological specimen, 2. Cryoultramicrotomy, 3. Cryotransfer including freeze-drying, 4. Energy dispersive X-ray microanalysis of the sections. The obtained X-ray spectra are then evaluated by the continuum method (Hall and Gupta, 1982; Statham, 1979) resulting in element concentrations in terms of mMol/kg dry weight. However, with respect to investigations on the distribution of diffusible ions depending on the physiological state of the cell, data in terms of wet weight concentration would be much more significant than the physiologically less important dry weight concentration. This requires the knowledge of the intracellular local water content. Some authors have approached this problem by measuring the continuum radiation of the X-ray spectrum in the frozen-hydrated and freeze-dried state and attributed the difference to the local water content (Gupta and Hall, 1981; Hall and Gupta, 1979; Saubermann et al., 1981; Zs -Nagy et al., 1982). This approach may be successful if sections with a thickness of at least 1/um or bulk specimens are analyzed. For ultrathin cryosections thinner than 200 nm as used for better spatial analytical resolution this method is not appropriate because of two reasons: 1. The contrast as seen in these frozen-hydrated cryosections in a scanning transmission electron microscope (STEM) is not sufficient for localization of ultrastructural details (Hagler and Buja, 1984; Zierold, 1983, 1985). 2. The electron dose necessary for the accumulation of X-ray spectra is very high, resulting in considerable mass loss and even destruction of the irradiated area which makes reliable measurements impossible (Zierold, 1983, 1985, 1986).

These problems prompted the development of an alternative method to estimate the local water content in ultrathin cryosections using their

freeze-dried equivalent. After freeze-drying, cryosections provide sufficient contrast in STEM and exhibit neither mass loss nor contamination by electron irradiation in a cold stage equipped STEM (Zierold, 1984a, 1986). In this paper the theoretical basis of the method will be described, followed by experimental validation. Then the application of the method will be illustrated using cultured fibroblast cells. In the discussion potentials and limitations of this method are compared with other techniques of mass measurement in the electron microscope.

Theoretical considerations

The basic experimental setup to be considered is schematically represented in Fig. 1: In a STEM the electron beam with the intensity I_0 irradiates the cryosection placed on an electron microscopical grid covered by a support film. The electron beam generates X-rays, a fraction of which are collected by an energy dispersive X-ray microanalysis system. Transmitted electrons arrive either at the central brightfield detector (B in Fig. 1) or at the annular darkfield detector (D in Fig. 1). The darkfield intensity after transmission of the support film is I_1, the darkfield intensity after transmission of the section placed on the support film is $I_1 + I_2$.

The evaluation of the X-ray spectra according to the continuum method (Hall and Gupta, 1982; Statham, 1979, 1981) is shown schematically in Fig. 2. The X-ray spectrum consists of peaks at characteristic energies, generated by elements with the atomic number Z higher than 10, above a broad continuum spectrum, also called white radiation, w. The continuum radiation w consists essentially of 3 portions: 1. the background b caused by interaction of the electron beam with the specimen. 2. The part f, caused by the interaction of the electron beam with the support film. 3. The extraneous radiation e, caused by interaction of uncollimated or scattered electrons with the grid, specimen holder, pole pieces, or other parts of the microscope column. For each energy interval the following equation holds:

$$w = b + f + e. \tag{1}$$

The main idea in the continuum evaluation method is, that b is proportional to the irradiated mass in the specimen. In a freeze-dried cryosection b is proportional to the remaining dry mass. As the area below the characteristic peak P of element a, P_a, is proportional to the number of atoms of this element in the section, the dry weight concentration C_a of the element a, usually given in mMol/kg dry weight, is given by:

$$C_a \sim P_a/b \tag{2}$$

By comparison with appropriate standard specimens containing known element concentrations, any unknown concentration C_a can be calculated.

$$C_a = \frac{(P_a/b) \cdot g}{F_a} \tag{3}$$

$$F_a = \frac{(P_a/b)_{st} \cdot g_{st}}{C_{st}} \tag{4}$$

The factor g takes into account that the P/b-value depends on the mean atomic number ($\bar{Z}$) of the analyzed area. For biological specimens g is proportional to $\bar{Z}$. The subscript st refers to the standard specimen.

The dry weight portion of a defined area in a freeze-dried cryosection can be measured by the darkfield intensity in STEM. As known from earlier reports, see e.g., Zeitler and Bahr (1962), Egerton (1982), Colliex et al. (1984), Carlemalm et al. (1985) the darkfield intensity in STEM can be described by the equation:

$$I = I_0(1 - \exp(-s \cdot \rho \cdot t)) \tag{5}$$

where s is a scattering parameter, depending on the particular electron optical system and the mean atomic number of the specimen, ρ = mass density of the specimen, t = specimen thickness. If $s \cdot \rho \cdot t$ is much smaller than 1, then equation (5) can be written as:

$$I = I_0 \cdot (s \cdot \rho \cdot t) \tag{6}$$

According to Fig. 1 the darkfield intensity from the film (subscript 1) is:

$$I_1 = I_0 \cdot (s_1 \cdot \rho_1 \cdot t_1) \tag{7}$$

The darkfield intensity from the specimen alone is:

$$I_2 = I_0 \cdot (s_2 \cdot \rho_2 \cdot t_2) \tag{8}$$

The relative darkfield intensity i for a specimen placed on a support film can be defined as:

$$(I_1 + I_2)/I_1 = i = 1 + \frac{s_2 \cdot \rho_2 \cdot t_2}{s_1 \cdot \rho_1 \cdot t_1} \tag{9}$$

The parameters s_1, ρ_1, and t_1 describing the support film can be assumed constant. In freeze-dried cryosections s_2 is assumed to be constant, because of the very similar elastic scattering parameters of dextran, used as standard, and most biological molecules present in cells and tissues. If also the specimen thickness t_2 can be kept constant, the relative darkfield intensity i is proportional to the mass density ρ_2. This means, in the case of a freeze-dried cryosection, that the relative darkfield intensity is proportional to the dry weight content d. A fully hydrated cryosection consists of the dry weight portion d and the liquid (or water) portion l with:

$$d + l = 1 \tag{10}$$

In freeze-drying the liquid portion vanishes by sublimation of ice. The water is substituted by vacuum which does not interact with the electron beam. Thus, by applying equations (9) and (10) the local water content, as present before freeze-drying, can be determined by measuring merely the relative darkfield intensity of a particular area in the freeze-dried cryosection.

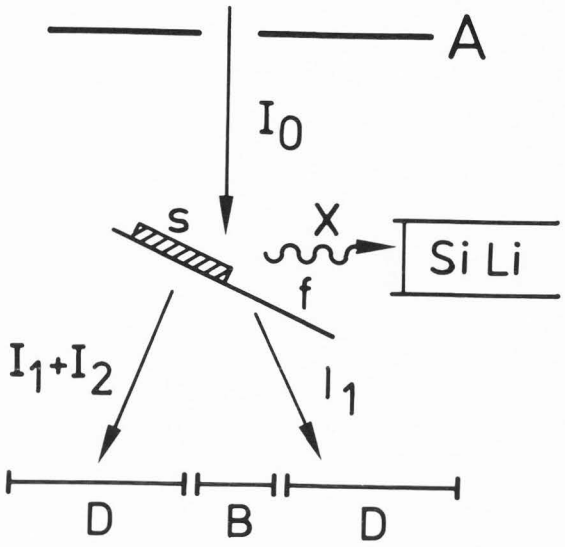

Fig. 1: Schematic drawing of the experimental setup: The primary electron beam passes the aperture A and scans the specimen s, here a cryosection, placed on the support film f, with the intensity I_0. X-rays (X) generated in the specimen are collected by the SiLi-detector (SiLi). The central brightfield detector (B) collects the unscattered and mainly inelastically scattered electrons. The majority of the elastically scattered electrons are collected by the annular darkfield detector (D). I_1 = darkfield intensity caused by the support film f, I_2 = darkfield intensity caused by the bare specimen.

The liquid concentration of the element a, called C_l, is then related to the dry weight concentration C_a by equation (10):

$$C_l = C_a \cdot \frac{d}{l} = C_a \cdot \frac{d}{1 - d} \qquad (11)$$

The wet weight concentration C_w is given by:

$$C_w = C_a \cdot d \qquad (12)$$

Experimental confirmation

The preparation of cryosections as used for this study has been described elsewhere (Zierold, 1982, 1984a, 1986). The freeze-dried cryosections were studied in a Siemens Elmiskop ST100F, a scanning transmission electron microscope equipped with a cryotransfer system and a cold stage. The temperature of the specimen in the electron microscope was kept at 138 K. X-ray spectra were analyzed by an energy dispersive SiLi detector

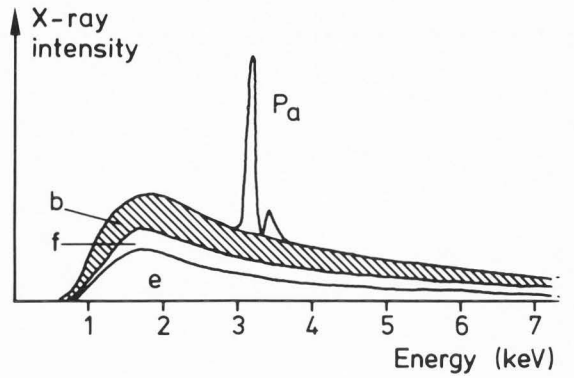

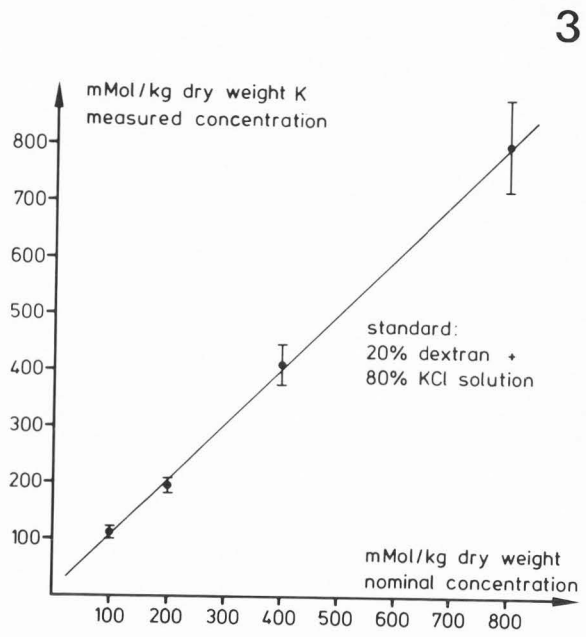

Fig. 2: Schematic drawing of a typical energy-dispersive X-ray spectrum: The element a causes a characteristic peak P_a above the white continuum spectrum w. The continuum is composed of the portion b, generated in the specimen, the portion f, generated in the support film, and the portion e, the extraneous radiation, caused elsewhere in the column of the electron microscope.

Fig. 3: Calibration curve for potassium, measured by X-ray microanalysis of freeze-dried cryosections from KCl-dextran solutions. The measured potassium concentration values are found after evaluation by the Link Quantem FLS program.

(nuclear semiconductor) and a Link microanalysis system using the Quantem FLS program for film and holder correction. The specimen was tilted by 30° towards the horizontally positioned X-ray detector

which was 12 mm apart. X-ray microanalysis was performed at 100 kV accelerating voltage with an objective aperture of 50/um and 4 nA beam current while scanning areas were varying usually from 7 x 11/um^2 to 70 x 110 nm^2.

Mixtures of 20% dextran and electrolyte solutions (NaCl, KCl, $MgSO_4$, KH_2PO_4, $CaCl_2$) in the concentration series 200, 100, 50, 25 mMol/l were used to prepare standard samples for the calibration of dry weight concentrations for Na, Mg, P, S, Cl, K, Ca. The cryosections were cut dry at nominal thickness of 70 nm. Due to compression caused by cutting the effective section thickness was about 100 nm. Only cryosections with ice crystal damage less than about 50 nm in diameter were used for X-ray microanalysis. Fig. 3 shows for example the linear relationship of the measured and theoretical K concentration, as obtained after evaluation and background correction by the Link Quantem FLS program. The energy interval between 4.2 and 6.2 keV was used for background correction.

The mass measurements with the annular darkfield detector were done with an objective aperture of 30/um and a beam current of 1.3 nA. The irradiation half angle was less than 10 mrad. The inner and outer half angles of the darkfield detector were 12 mrad and 94 mrad, respectively. The measurements in one particular cryosection and in the related film area were performed at constant photomultiplier and amplifier settings. For calibration measurements dextran was mixed with water in weight concentrations between 5% and 50% and prepared in the same way as described above.

The linear relationship between the relative darkfield intensity and the irradiated mass as suggested by equation (9) was tested by ruptured support films which partly overlapped each other several times. This is shown by Fig. 4. Fig. 5 shows the results obtained from the cryosections with varying dextran content. The relative darkfield intensity values are in the same range as in Fig. 4, supporting the assumption of the linear relationship between mass and relative darkfield intensity. The calibration line in Fig. 5 can be expressed by the equation

$$d = d_0 \cdot (i - 1) \qquad (13)$$

The calibration factor d_0 depends on the particular electron optical conditions. In the case described here is $d_0 = 0.25$. This method allows the measurement of the local dry weight content between 0.05 and 0.5, respectively the local water content between 0.5 and 0.95 with an accuracy of 8 to about 15% as indicated by the bars in Fig. 5. The spatial resolution is determined by the electron probe diameter, the ice crystal damage and the microroughness of the sections. The scanned area should be larger than the ice crystal size in the section in order to average mass thickness differences caused by ice crystal damage. The maximal ice crystal damage tolerated in freeze-dried cryosections for X-ray microanalysis is about 50 nm. Cryosections undergo compression during cutting which results in unidirectional thickness variations with a period of 150-300 nm (Zierold, 1984b). Thus, the spatial resolution of the STEM darkfield method to measure the local water content ranges from 50 nm to 300 nm depending on the morphology of the particular cryosection.

Application to biological cells

The method was applied to a suspension of fibroblast cells. Fig. 6 shows a freeze-dried cryosection of a fibroblast cell in the ratio image contrast (brightfield/darkfield). Fig. 7 shows the corresponding darkfield image. The contrast in Figs. 6 and 7 is essentially determined by the darkfield signal, and this depends on the mass thickness. In Fig. 6 the brightness is approximately proportional to the local water content, in Fig. 7 the brightness represents the local dry mass. Table 1 summarizes dry weight and wet weight concentrations of elements found by X-ray microanalysis and STEM darkfield measurements in different subcellular compartments. The water content of the nucleus is slightly higher than in the cytoplasm. As expected, mitochondria contain more dry weight than the cytoplasm and the nucleus. The differences in the dry weight element concentrations with respect to these three different compartments are reduced after relating the element concentrations to the local water content. This finding has to be studied in more detail by future experiments.

In principle, also the ion concentration in the extracellular liquid can be determined. However, the very low dry weight concentration causes very high standard deviations in the calculation.

The conversion of dry weight concentrations into wet weight concentrations is just a formal procedure. The element concentration values in Table 1 are related either to the dry matrix or to the water content in the cell without respect to the actual state of these atoms. The data give no information on activity and do not prove if and to which amount the elements in the living cell are dissolved in the water or bound to organic molecules.

Discussion

One reason for the wide application of the continuum method in quantitative evaluation of X-ray spectra in biological microanalysis is that it is based on the measurement of a relative quantity (p/b). No absolute quantities have to be determined (Marshall and Hall, 1968; Hall and Gupta, 1979; Gupta and Hall, 1981). Neither the amount of elements nor the organic dry mass have to be determined absolutely. Indeed, the measurement of any absolute mass content by X-ray analysis is complicated, because of the different contributions to the continuum radiation as described by equation (1) and schematically illustrated by Fig. 2. There are many reports in the literature on the problem of how to separate clearly the different continuum portions in order to obtain the absolute background b caused by the specimen (Goldstein and Williams, 1978; Statham, 1979; Roomans and Kuypers, 1980; Grote and Fromme, 1981; Heinrich, 1982; Nicholson et

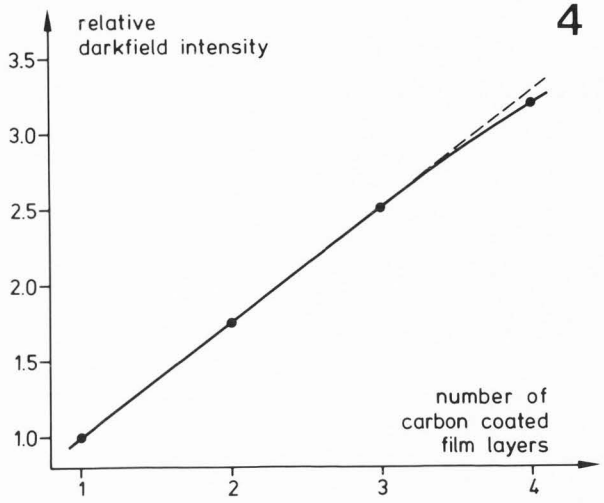

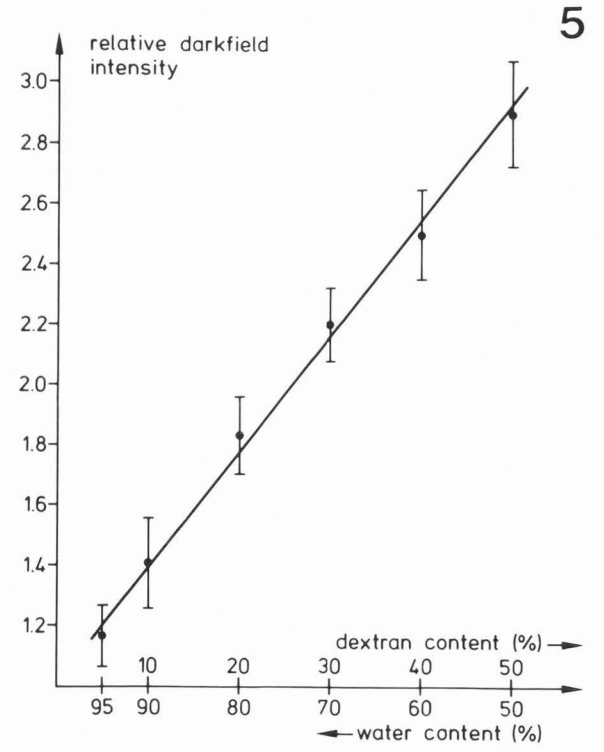

Fig. 4: Relative darkfield intensity, obtained from carbon-coated film layers.

Fig. 5: Relative darkfield intensity obtained from freeze-dried cryosections of dextran-water solutions with varying dry mass content.

Fig. 6: STEM ratio image (brightfield/darkfield) of a cryosection of a fibroblast cell in suspension. C = cytoplasm, M = mitochondria, N = nucleus. Assuming the validity of equation (10), the brightness represents the water content. Bar = 1/um.

Fig. 7: STEM darkfield image of the section shown in Fig. 6. Assuming the validity of equation (10), the brightness represents the dry mass content. Bar = 1/um.

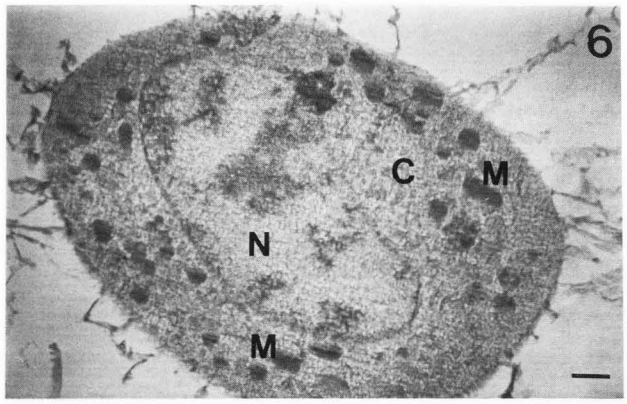

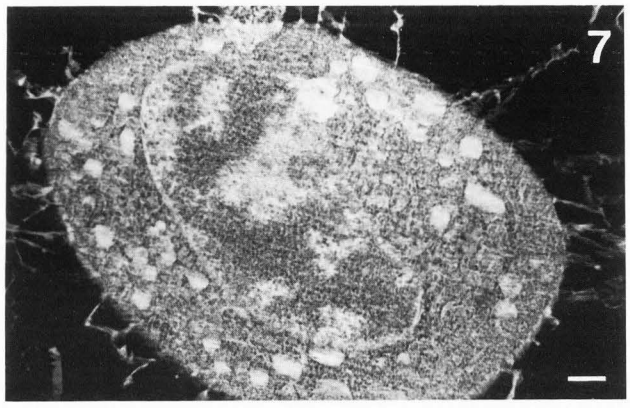

Table 1

$\bar{x}$+S.D. n=10	nucleus	cytoplasm	mitochondria
$\bar{d}$	0.14 ± 0.03	0.17 ± 0.04	0.33 ± 0.10
Na	89 ± 24 12 ± 3	61 ± 11 10 ± 3	33 ± 8 11 ± 4
Mg	77 ± 19 11 ± 5	68 ± 21 12 ± 6	52 ± 14 20 ± 12
P	548 ± 168 77 ± 33	360 ± 83 59 ± 19	234 ± 73 82 ± 32
S	249 ± 61 35 ± 12	176 ± 28 29 ± 10	140 ± 36 50 ± 27
Cl	141 ± 26 19 ± 5	124 ± 60 19 ± 7	20 ± 7 7 ± 3
K	626 ± 162 87 ± 32	372 ± 83 61 ± 21	165 ± 60 60 ± 42
Ca	---	---	---

Element distribution in different compartments of fibroblast cells in suspension. $\bar{d}$ = mean dry weight portion. The upper values of element concentrations are dry weight concentrations in mMol/kg dry weight, the lower values are wet weight concentrations in mMol/kg wet weight. $\bar{x}$ = mean value, S.D. = standard deviation, n = number of measured cells.

al., 1982; Ryan et al., 1984; Warner et al., 1985). Linders et al. (1981, 1982a, 1984) have compared different methods of mass measurement in the electron microscope. They conclude that the data obtained from the transmitted electron signal are more accurate than those derived from the X-ray analysis. Extraneous effects on the transmitted electron signal are negligibly small in comparison with the situation in X-ray analysis. This could be confirmed by experiments on freeze-dried cryosections in STEM.

Recently, Ingram and Ingram (1983) have presented an X-ray analytical method to measure the intracellular water distribution by use of sections of freeze-dried and embedded biological material. They start from the consideration that during the embedding process the intracellular water is replaced by plastic. After dissolving an element in the fluid plastic which is not expected in the biologial specimen - in this particular case bromine - the specimen is embedded in this labeled plastic. The bromine concentration measured by X-ray microanalysis is then a measure of the local water content. However, in some cases the embedding step might influence the element distribution (Roos and Barnard, 1985). Therefore, the possibility of element redistribution by plastic embedding has to be considered carefully in each particular biological investigation.

Electron signals from the specimen provide X-ray independent measures for the local dry mass. In principle, backscattered electrons can be used for the determination of the local dry mass (Niedrig, 1978; Linders, et al., 1982a; Linders and Hagemann, 1983). However, this method requires specimens, which are much thicker than ultrathin cryosections. The backscattered electron intensity expected from ultrathin cryosections is not sufficient to provide reliable mass measurements.

The transmitted electrons signal is well known to account for local mass thickness information. Originally, the electron beam attenuation according to Beer's law was used as a measure for local mass thickness in the electron microscopical specimen (Marton and Schiff, 1941; Burge and Silvester, 1959; Zeitler and Bahr, 1962, 1965; Bahr and Zeitler, 1965; Wall, 1979; Pozsgai and Barna, 1983; Siklós, 1983). This method was applied very often to determine the local mass thickness of biological specimens by measuring the transmitted electron intensity by use of microdensitometry of the irradiated photographic film (Linders et al., 1982a and b, 1985) or by measuring the STEM brightfield intensity (Halloran et al., 1978). However, the brightfield signal in STEM is composed by the inelastically scattered and unscattered electrons. The latter reduce the contrast obtained from two areas with different mass thickness.

The annular darkfield detector in STEM very efficiently collects electrons scattered elastically by the specimen (Langmore et al., 1973; Engel, 1978; Wall, 1979; Crewe, 1983). Freeman and Leonard (1981), Mosesson et al. (1981), Di Capua et al. (1982), Johnson and Wall (1983), and Steven et al. (1983) have used the relationship between STEM darkfield and mass thickness to determine the molecular weight of biological macromolecules and isolated vesicles. Experiments on ultrathin freeze-dried cryosections have shown that a specimen contrast causing the darkfield intensity to change by the factor of 3 induces a brightfield intensity difference of merely 25%. This example illustrates the advantage of STEM darkfield measurements for mass thickness determination with respect to accuracy and precision, as already evident from comparison of STEM imaging conditions for unstained biological sections (Hosoi et al., 1981a; Zierold, 1985).

Measurements and calculations by Egerton (1982), Engel and Reichelt (1984), Reichelt and Engel (1984, 1985), Reichelt et al. (1984, 1985), Colliex et al. (1984), and Carlemalm et al., (1985) indicate that in a rather small range of mass thickness the electron energy loss signal provides mass information with similar accuracy. However, the electron energy loss signal declines at considerably smaller mass thickness than the annular darkfield signal, until even contrast reversal occurs. Lamvik (1978) has measured the mass per unit length of muscle thick filaments by using the inelastically scattered electrons. Hosoi et al. (1981b) have studied the specific thickness of critical-point-dried cultured fibroblast cells by electron energy loss spectroscopy (EELS). Leapman et al. (1984) recommend EELS as an X-ray microanalytically independent method to determine the local mass in thin biological specimens. However, it remains to be clarified in future experiments whether the mass thickness of freeze-dried cryosections is thin enough, even in electron dense compartments such as mitochondria or dense granules, in order to avoid multiple scattering which causes deviations from the linearity between mass thickness and EELS signal.

Thus, the STEM darkfield intensity measurement turns out to be an efficient and easy method for local mass determination in freeze-dried cryosections. The high sensitivity for variations in the local water content is based on the fact that freeze-drying substitutes water by vacuum with the electron scattering cross section zero, distinctly different from the scattering cross section of the remaining dry mass. A further advantage of this method is that only two short measurements are required: The darkfield intensity from the cryosection ($I_1 + I_2$) and from the film only (I_1). Since the mass is derived from the ratio $i = (I_1 + I_2)/I_1$ the method is independent of longtime variations in the intensity of the primary electron beam, the sensitivity of the scintillator crystal, the characteristics of the photomultiplier and the amplifier.

However, a critical parameter in this method is the section thickness t_2 as can be seen in equation (9). Despite the first results presented in Table 1 further experience is required to judge whether the quality of cryosections as produced by present cryoultramicrotomy is sufficient for reliable mass measurements. Cryosections are known to be compressed by the sectioning process as can be seen very often by unidirectional compression lines (Zierold, 1984b). It is unknown whether this deformation occurs uniformly in compartments with different water content. In any case the reproducible section thickness is a prerequisite for reliable mass measurements in the electron microscope.

Conclusions

Freeze-dried ultrathin cryosections of biological cells contain information on the distribution of elements and organic mass. Dry weight concentrations of elements are measured by energy dispersive X-ray microanalysis and evaluated by the continuum method. Assuming that the dry mass distribution represents the complementary water distribution, the local water portion can be determined by relative darkfield intensity measurements in STEM. The combination of both methods provides local wet weight concentrations of elements. Both methods derive advantage from the fact that they are based on the measurement of relative physical quantities. Thus, inaccuracies caused by instrumental parameters are reduced. However, the reliable determination of the local mass and water content by relative darkfield intensity measurements requires cryosections of reproducible thickness.

Acknowledgement

I thank Miss S. Dongard for her excellent technical assistance.

References

Bahr GF, Zeitler E. (1965). The determination of the dry mass in populations of isolated particles. Lab. Invest. 14(6), 217-239.

Burge RE, Silvester NR. (1959). The measurement of mass, thickness and density in the electron microscope. J. Biophys. Biochem. Cytol. 8, 1-11.

Carlemalm E, Colliex C, Kellenberger E. (1985). Contrast formation in electron microscopy of biological material. Advances in Electronics and Electron Physics 63, 269-334.

Colliex C, Jeanguillaume C, Mory C. (1984). Unconventional modes for STEM imaging of biological structures. J. Ultrastruct. Res. 88, 177-206.

Crewe AV. (1983). High resolution scanning transmission electron microscopy. Science 221, 325-331.

Di Capua E, Engel A, Stasiak A, Koller Th. (1982). Characterisation of complexes between recA protein and duplex DNA by electron microscopy. J. Mol. Biol. 157, 87-103.

Egerton RF. (1982). Thickness dependence of the STEM ratio image. Ultramicroscopy 10, 297-299.

Engel A. (1978). Molecular weight determination by scanning transmission electron microscopy. Ultramicroscopy 3, 273-281.

Engel A, Reichelt R. (1984). Imaging of biological structures with the scanning transmission electron microscope. J. Ultrastruct. Res. 88, 105-120.

Freeman R, Leonard KR. (1981). Comparative mass measurement of biological macromolecules by scanning transmission electron microscopy. J. Microsc. 122, 275-286.

Goldstein JI, Williams DB. (1978). Spurious X-rays produced in the scanning transmission electron microscope. Scanning Electron Microsc. 1978; I:427-434.

Grote M, Fromme HG. (1981). Specimen chamber geometry - A possible source of error in quantitative X-ray microanalysis in STEM. J. Electron Microsc. 30(4), 359-361.

Gupta BL, Hall TA. (1981). The X-ray microanalysis of frozen-hydrated sections in scanning electron microscopy: An evaluation. Tissue Cell 13(4) 623-643.

Hagler HK, Buja LM. (1984). New techniques for the preparation of thin freeze dried cryosections for X-ray microanalysis. in: The Science of Biological Specimen Preparation for Microscopy and Microanalysis, Revel J-P, Barnard T, Haggis GH, Bhatt SA (eds.), Proc. of the 2nd Pfefferkorn Conference 1983, SEM Inc., AMF O'Hare,IL (USA), 161-166.

Hall TA, Gupta BL. (1983). The localization and assay of chemical elements by microprobe methods. Quart. Rev. Biophys. 16(3) 279-339.

Hall TA, Gupta BL. (1979). EDS quantitation and application to biology. in: Introduction to Analytical Electron Microscopy, Hren JJ, Goldstein JI, Joy DC (eds.) Plenum Press, New York and London, 169-197.

Hall TA, Gupta BL. (1982). Quantification for the X-ray microanalysis of cryosections. J. Microsc. 123, 333-345.

Halloran BP, Kirk RG, Spurr AR. (1978). Quantitative electron probe microanalysis of biological thin section: The use of STEM for measurements of local mass thickness. Ultramicroscopy 3, 175-184.

Heinrich KFJ. (1982). The accuracy of quantitation in X-ray microanalysis, particularly of biological specimens. Scanning Electron Microsc. 1982; I:281-287.

Hosoi J, Inoue M, Sasaki H, Kokubo Y, Johansen BV. (1981a). Observation of low contrast biological specimens by annular type STEM darkfield method using signal processor. J. Electron Microsc. 30(2), 154-157.

Hosoi J, Oikawa T, Inoue M, Kokubo Y, Hama K. (1981b). Measurement of partial specific thickness (net thickness) of critical-point-dried cultured fibroblast by energy analysis. Ultramicroscopy 7(2), 147-153.

Ingram MJ, Ingram FD. (1983). Electron microprobe calibration for measurement of intracellular water. Scanning Electron Microsc. 1983; III:1249-1254.

Johnson KA, Wall JS. (1983). Structure and molecular weight of the dynein ATPase. J. Cell Biol. 96, 669-678.

Lamvik MK. (1978). Muscle thick filament mass measured by electron scattering. J. Mol. Biol. 122, 55-68.

Langmore JP, Wall J, Isaacson MS. (1973). The collection of scattered electrons in darkfield electron microscopy. I. Elastic scattering. Optik 38, 335-350.

Leapman RD, Fiori CE, Swyt CR. (1984). Mass thickness determination by electron energy loss for quantitative X-ray microanalysis in biology. J. Microsc. 133, 239-253.

Linders PWJ, Hagemann P. (1983). Mass determination of thin biological specimens using backscattered electrons. Application in quantitative X-ray microanalysis on an automated STEM system. Ultramicroscopy 11, 13-20.

Linders PWJ, Stols ALH, Stadhouders AM. (1981). Quantitative electron probe X-ray microanalysis of thin objects using an independent mass determination method. Micron 12, 1-4.

Linders PWJ, Stols ALH, Van de Vorstenbosch RA, Stadhouders AM. (1982a). Mass determination of thin biological specimens for use in quantitative electron probe X-ray microanalysis. Scanning Electron Microsc. 1982; IV:1603-1615.

Linders PWJ, Zahniser DJ, Stols ALH, Stadhouders AM. (1982b). Improved mass determination of isolated biological objects by transmission electron microscopy and scanning microdensitometry. J. Histochem. Cytochem. 30(7), 637-644.

Linders PWJ, Van de Vorstenbosch RA, Smits HTJ, Stols ALH, Stadhouders AM. (1984). Absolute quantitative electron microscopy of thin biological specimens by energy-dispersive X-ray microanalysis and densitometric mass determination. Analytica Chimica Acta 160, 57-67.

Linders PWJ, Van de Vorstenbosch RA, Stadhouders AM. (1985). Quantitative electron probe X-ray microanalysis and densitometric mass determination of individual rat blood platelets. J. Histochem. Cytochem. 33(3), 185-190.

Marshall DJ, Hall TA. (1968). Electron-probe X-ray microanalysis of thin films. Brit. J. Appl. Phys. (J. Phys. D), Ser. 2, Vol. 1, 1651-1656.

Marton L, Schiff LI. (1941). Determination of object thickness in electron microscopy. J. Appl. Phys. 12, 759-765.

Mosesson MW, Hainfeld J, Wall J, Haschemeyer RH. (1981). Identification and mass analysis of human fibrinogen molecules and their domains by scanning transmission electron microscopy. J. Mol. Biol. 153, 695-718.

Nicholson WAP, Gray CC, Chapman JN, Robertson BW. (1982). Optimizing thin film X-ray spectra for quantitative analysis. J. Microsc. 125, 25-40.

Niedrig H. (1978). Physical background of electron backscattering. Scanning 1, 17-34.

Pozsgai I, Barna A. (1983). Wavelength-dispersive microanalysis in the transmission electron microscope. Scanning Electron Microsc. 1983; II:585-601.

Reichelt R, Carlemalm E, Engel A. (1984). Quantitative contrast evaluation for different scanning transmission electron microscope imaging modes. Scanning Electron Microsc. 1984; III:1011-1021.

Reichelt R, Engel A. (1984). Monte Carlo calculations of elastic and inelastic electron scattering in biological and plastic materials. Ultramicroscopy 13, 279-293.

Reichelt R, Carlemalm E, Villiger W, Engel A. (1985). Concentration determination of embedded biological matter by scanning transmission electron microscopy. Ultramicroscopy 16, 69-80.

Reichelt R, Engel A. (1985). Quantitative scanning transmission electron microscopy in biology. J. Microsc. Spectrosc. Electron. 10, 491-498.

Rick R, Dörge A, Thurau K. (1982). Quantitative analysis of electrolytes in frozen dried sections. J. Microsc. 125, 239-247.

Roomans GM, Kuypers AJ. (1980). Background determination in X-ray microanalysis of biological thin sections. Ultramicroscopy 5, 81-83.

Roomans GM, Wei X, Sevéus L. (1982). Cryoultramicrotomy as a preparative method for X-ray microanalysis in pathology. Ultrastruct. Pathol. 3, 65-84.

Roos N, Barnard T. (1985). A comparison of subcellular element concentrations in frozen-dried, plastic-embedded, dry-cut sections and frozen-dried cryosections. Ultramicroscopy 17, 335-343.

Ryan KG, Flower NE, Presland MR. (1984). Specimen holder design for X-ray microanalysis of thin films in the TEM: reduction of spurious X-rays. J. Microsc. 134, 281-289.

Saubermann AJ, Beeuwkes III R, Peters PD. (1981). Application of scanning electron microscopy to X-ray analysis of frozen-hydrated sections. II. Analysis of standard solutions and artificial electrolyte gradients. J. Cell Biol. 88, 268-273.

Siklós L. (1983). Assembly and reliability of an X-ray microanalyser system with a possibility for independent mass measurement. Acta Biochim. Biophys. Acad. Sci. Hung. 18(3-4), 211-222.

Somlyo AV, Shuman H, Somlyo AP. (1977). Elemental distribution in striated muscle and the effects of hypertonicity. Electron probe analysis of cryosections. J. Cell Biol. 74, 828-857.

Somlyo AP, Shuman H. (1982). Electron probe and electron energy loss analysis in biology. Ultramicroscopy 8, 219-234.

Statham PJ. (1979). Measurement and use of peak-to-background ratios in X-ray analysis. Mikrochimica Acta. 8, 229-242.

Statham PJ. (1981). X-ray microanalysis with Si (Li) detectors. J. Microsc. 123, 1-23.

Steven AC, Hainfeld JF, Wall JS, Steer CJ. (1983). Mass distributions of coated vesicles isolated from liver and brain: Analysis by scanning transmission electron microscopy. J. Cell Biol. 97, 1714-1723.

Wall JS. (1979). Mass measurements with the electron microscope. Scanning Electron Microsc. 1979; II:291-302.

Warner RR, Meyers MC, Taylor DA. (1985). Inaccuracies with the Hall technique due to continuum variation in the analytical microscope. J. Microsc. 138, 43-52.

Wendt-Gallitelli M-F, Wolburg H. (1984). Rapid freezing, cryosectioning, and X-ray microanalysis on cardiac muscle preparations in defined functional states. J. Electron Microsc. Tech. 1, 151-174.

Zeitler E, Bahr GF. (1962). A photometric procedure for weight determination of submicroscopic particles quantitative electron microscopy. J. Appl. Phys. 33(3), 847-853.

Zeitler E, Bahr GF. (1965). Contrast and mass thickness. Lab. Invest. 14(6), 208-216.

Zierold K. (1982). Preparation of biological cryosections for analytical electron microscopy. Ultramicroscopy 10, 45-53.

Zierold K. (1983). X-ray microanalysis of frozen-hydrated specimens. Scanning Electron Microsc. 1983; II:809-826.

Zierold K. (1984a). Experiences in X-ray microanalysis of freeze-dried cryosections. Scanning Electron Microsc. 1984; IV:1867-1874.

Zierold K. (1984b). The morphology of ultrathin cryosections. Ultramicroscopy 14, 201-209.

Zierold K. (1985). Contrast of biological cryosections in scanning transmission electron microscopy. J. Microsc. 140, 65-71.

Zierold K. (1986). Preparation of cryosections for biological microanalysis. in: Proceedings of the 4th Pfefferkorn Conference on the Science of Biological Specimen Preparation 1985, Becker R, Boyde A, Müller M, Wolosewick J (eds.), Scanning Electron Microscopy Inc., AMF O'Hare, IL, 119-127.

Zs -Nagy I, Lustyik G, Bertoni-Freddari C. (1982). Intracellular water and dry mass content as measured in bulk specimens by energy-dispersive X-ray microanalysis. Tissue Cell 14(1), 47-60.

Discussion with Reviewers

F.D. Ingram: The Rutherford scattering cross section is a function of Z^2/E^2. Does this not imply that the scattering coefficient, s_2, in eq. (8) is more a function of Z than sample density? Assuming uniform sample thickness, how can it be determined that the electron image contrast differences among dried cytoplasmic material, mitochondria, and nuclear material is a function of water content and not Z?

R. Reichelt: The derivation of eq. (9) from eq. (5) is not clear to me. According to the paper by Colliex et al. (1984) you mentioned, on page 189, the annular detector (AD) signal is given for very thin specimen as:

$$I_{AD} = I_0 (1-\exp(-t/\Lambda_e))$$

where Λ_e is the mean free path between two sequential elastic events. Λ_e can be estimated by the relation $\Lambda_e = 1/N\sigma_e$ where Λ_e represents the elastic electron scattering cross section, depending only on the electron energy and the atomic number, and N is the number of atoms per volume. N is given as $N = \rho \cdot L/A$ (where ρ: mass density of the specimen, L: Avogadro's number, A: atomic weight; cf. Zeitler & Bahr, Exper. Cell Res. 12 (1957) p. 48). It means $t/\Lambda_e = \sigma_e(L/A)\rho \cdot t$ and comparison with your eq. (6) shows that the scattering parameter s is given by $s = \sigma_e \cdot L/A$. In case of specimens composed of different atoms with various atomic numbers the mean values of σ_e and A have to be used (Reichelt & Engel, (1984); Colliex et al., (1984)). Using typical values for σ_e and A (cf. Tab. IB, Colliex et al., 1984), s depends on the composition of the volume irradiated (for example: Carbon: $4.14 \cdot 10^4$ cm^2/g; protein: $3.83 \cdot 10^4$ cm^2/g; ice: $3.32 \cdot 10^4$ cm^2/g). In your eq. (8) identical s for areas with different composition is used. Could you make a statement to that?

Author: The scattering parameter s depends on the atomic number Z. However, in the case of freeze-dried sections of biological cells a mean value of s for the different intracellular compartments can be tolerated.
In the paper of Carlemalm et al. (1985), cited in the text, Table II, p. 288 several values of s are given. They are (in units of m^2/g) for carbohydrate (dextran) 3.55, protein 3.64, lipid 3.76, nucleic acid 3.91. With regard to these data the correction of the values measured in cell nuclei (Tab. 1) by the factor 0.91 would be appropriate.

M.K. Lamvik: In equation (6) you assume that $s \cdot \rho \cdot t$ is much smaller than one (i.e., the specimens are thin), but near the end of your paper you suggest that the cryosections are too thick to allow the use of an electron energy loss spectrometer to measure them. Since the inelastic mean free path is only about half the elastic mean free path for typical organic specimens, why does the same thickness lead to such different suggestions for the two methods? What is the value of the elastic mean free path $(1/s \cdot \rho)$ that you have measured for your cryosections?

F.D. Ingram: What are the requirements on sample thickness and accelerating voltage imposed by the factor ρ, s and t of equation (8)?

Author: At 100 kV the scattering parameters of dextran (ρ = 1.5 g/cm^3) is 3.55 m^2/g (Carlemalm et al., 1985, cited in the text). The elastic mean free path in a freeze-dried cryosection of a solution composed of 50% dextran and 50% water is then approximately 400 nm. This is well above the section thickness of 100 nm. However, in the case of electron-dense particles containing heavy elements multiple scattering cannot be excluded. The linear relationship between relative darkfield intensity and dry weight portion depends on the condition $s \cdot \rho \cdot t \ll 1$. This means that the section thickness t must be distinctly smaller than the elastic mean free path $(1/s \cdot \rho)$. The elastic mean free path increases with the accelerating voltage.

P. Linders: The assumption of constant section thickness and equation (10) require for any measured relative darkfield intensity value i the non aqueous part to have a uniform or constant density. For a constant liquid fraction, the dry mass density must be constant. This puzzles me; what about granular inclusions or dense particles? Please clarify.

Author: According to equation (9) the relative darkfield intensity measures the mass thickness $\rho \cdot t$. Provided that the section thickness is constant and the scattering parameter s of the dry matrix is similar to that of the standard (dextran), then the measured relative darkfield intensity value i is proportional to the dry weight portion d. The liquid portion l decreases with increasing dry weight portion d. For example condensed protein structures such as mitochondria

turn out to have higher dry weight portions than e.g. cytoplasmic areas, and consequently the liquid portion l is usually lower in mitochondria than in the cytoplasm. However, the dry weight portion of granules with a scattering parameter distinctly different from that of the standard has to be evaluated by use of an atomic number-dependent correction factor, as mentioned above.

M.K. Lamvik: You define the "relative darkfield intensity" as $i=(I_1+I_2)/I_1$, where I_1 is the intensity recorded from the substrate film. Yet in Fig. 5, the intercept gives zero intensity for a cryosection of 100% water content, implying that the data have been renormalized to no longer include the substrate film. Could you describe this part of your method in more detail, relating it to the measurement of an unknown cryosection?

Author: As can be seen in Fig. 5, for a section, which had 100% water content in the frozen-hydrated state, i will be 1, in agreement with equation (9).

M.K. Lamvik: If you measured an adipocyte where the fat droplet had $\rho < 1$, it appears that your method would indicate a water content greater than 100%. How sensitive is your method to differences in density?

Author: This would not be the case. As can be seen by equation (9) and by Fig. 5, any dry weight portion greater than zero causes a relative darkfield intensity value i greater than 1. The accuracy of the darkfield signal depends on the photomultiplier noise. The error in the darkfield intensity measurements is between 5 and 10%, which results in the absolute error of ± 0.02 in the determination of the dry weight portion d.

F.D. Ingram: Precisely how sensitive is the method to variations in section thickness: a) point-to-point within the sample, and b) section-to-section?

M.K. Lamvik: The errors in your proposed method are estimated as 8 to 15%, based on error bars in Fig. 5. Could you describe how the error bars were determined?

Author: The calibration curve in Fig. 5 is based on at least 6 measurements at each dextran concentration used (5%, 10%, 20%, 30%, 40%, 50%). Each measurement was done in a different section. There was negligible variation in one and the same section. The error bars drawn in Fig. 5 represent the standard deviation of the data obtained from at least 6 different sections.

R. Reichelt: How is the thickness of ultrathin cryosections estimated? What is the extent of local thickness variation?

M.K. Lamvik: As you point out, your method is accurate only if the section thickness is constant. It seems difficult to cut a series of cryosections that have equal thickness within 10%. How do you measure the thickness of the cryosections? What variations in thickness have you observed?

F.D. Ingram: How much section-to-section thickness variation is encountered in samples sectioned at low temperature?
How does the well-documented shrinkage that accompanies freeze-drying of tissues affect interpretation of your data, and in particular, eqs. 9 and 10.?

H.K. Hagler: How much uncertainty would be introduced in the wet weight concentrations if the section thicknesses were only known to be within 30%? Please discuss how this would affect measurements taken from sections produced at different times.

Author: The section thickness was not measured. All sections were cut by the Reichert FC4 Ultracut cryoultramicrotome at a temperature below 170K. The advance settings were kept constant at 70 nm. The obtained sections appeared clear and similar by light microscopic observation in the cryoultramicrotome chamber. Also the electron optical density of sections on the same grid seemed to be approximately the same as observed by STEM darkfield contrast, in particular in the standards. Some few curled sections allowed to measure their edge width directly in STEM, which was found to vary between 90 nm and 120 nm. Variations in section thickness were caused partly by inhomogeneous compression caused by cutting. Freeze-drying-induced shrinkage was probably uniform in sections of standards containing the same dry weight concentration, however, in sections of cellular material the possibly inhomogeneous shrinkage could be one source of error in the evaluation of the dry weight portion.
As can be seen by equation (9), the relative darkfield intensity i is proportional to the product $\rho \cdot t$. Therefore, any thickness variation will cause a proportional variation of the dry weight portion d. Thickness variations in sections cut at different times were not studied explicitly. However, the standard sections containing different dry weight content for establishing the calibration curve of the relative darkfield intensity (Fig. 5) were prepared at several days. The variation of the measured data is within the error bars, shown in Fig. 5. Further experiments are required to test whether the thickness of cryosections from cellular material can be kept constant on a long time scale.

P. Linders: The maximum ice crystal size allowed in the analyses is 50 nm diameter. In the smallest scan frame (70 x 110 nm^2), one such crystal occupies ca. 25% of the area (and volume ?). To what extent have such crystals influenced your measurement accuracy and precision?

Author: If the size of the electron probe is about the same as the ice crystal damage, then large intensity variations are observed because of the high effective thickness variations between holes left by the sublimed ice and condensed dry matrix segregations. If the probe size is much larger than the ice crystal damage, then the signal is

averaged over these thickness variations.

F.D. Ingram: How thick were the films used for Fig. 4? Because Fig. 4 provides interesting data on the region of linearity for the method, it is of some interest to know the thickness of the film in absolute units.

Author: The film consisted of Pioloform F^R coated by a 20 nm thick layer of carbon. The total thickness of the film was measured to be about 50 nm according to imaging of contamination spots on the warm support film at different tilt angles.

F.D. Ingram: How sensitive is the method to calibration of the photomultiplier signal? How is the relationship checked on a day-to-day basis. Is the signal linearity dependent upon microscope parameters and signal levels?

Author: Test measurements under different amplification conditions have shown that the linearity of the curve shown in Fig. 4 did not vary in the observed amplification range. Long time variations in the signal stability have to be checked in the future.

R. Reichelt: I am confused by your interpretation that Fig. 4 proves the linear relationship between mass and relative darkfield intensity i. Using eq. (9) to evaluate i of a partly overlapped ruptured support film, one gets $i = 1+t_2/t_1$. For one layer, i.e. $t_2 = 0$, eq. (9) reveals $i = 1$ in agreement with Fig. 4. For two layers, i.e. $t_2 = t_1$, eq. (9) gives $i = 2$ in contrast to 1.75 shown in Fig. 4. Finally, for three layers I expect $i = 3$ in contrast to 2.5. This deviation may indicate already the influence of plural scattering. Do you agree to my guess?

P. Linders: Fig. 4 is supposed to illustrate the linear relation between the relative darkfield signal and the dry mass. How do you explain that with two (or three) film layers the relative darkfield signal is not equal to two (or three) times the signal from one film layer?

Author: Actually, the darkfield signal is superimposed on a bias signal in such a way that the darkfield intensity $I = a+k\cdot t$, where a = bias signal, t = specimen thickness and k = proportionality constant. Therefore, n film layers generate the relative darkfield signal

$$i = \frac{a+n\cdot k\cdot t}{a+k\cdot t} = 1 + \frac{(n-1)\cdot k\cdot t}{a+k\cdot t}$$

This signal is still proportional to the number of film layers as shown in Fig. 4. I do not expect multiple scattering effects in the observed thickness range, except for the upper right end of the curve shown in Fig. 4.

R. Reichelt: How can one interpret the results of eq. (11) using the following values for d?

d = 0.5 then $C_1 = C_a$, and
d = 1.0 then $C_1 \rightarrow \infty$, i.e. not defined.

Author: d = 0.5 or $C_1 = C_a$ means that dry weight portion and liquid portion are equal. Consequently, the dry weight concentration equals the liquid concentration. The wet weight concentration is 1/2 of the dry weight concentration.
If d = 1, then the liquid concentration is 0. The specimen was completely dry already before freeze-drying. Consequently, the liquid concentration C_1 is not defined.

P. Linders: Is the contrast in Fig. 6, the ratio-contrast, independent of the relative amplification and dc level shifts of both brightfield and darkfield signals? If not, almost any contrast can be generated from a given specimen, and then Fig. 6 certainly does not represent a "water picture". Please comment.

Author: Of course, the contrast depends on the amplification of the brightfield and darkfield signals. The brightness represents the water content only qualitatively, not quantitatively.

M.K. Lamvik: Your data have been presented as relative intensities. Other units would make comparisons more convenient. Assuming the brightfield (I_b) and darkfield (I_d) detectors have equal gains and the specimens are thin enough, the elastic signal I_e/I_0 is roughly approximated by $I_d/(I_b+I_d)$. Could you say what one unit of "relative darkfield intensity" in Figs. 4 and 5 would be in terms of this darkfield-to-total ratio?

Author: In principle, it should be possible to use also the darkfield-to-total ratio for mass measurements in STEM. However, this requires two measurements for each point instead of one (only the darkfield), as described. Usually, the brightfield and darkfield amplifications are different. Therefore, I am not able to easily convert the relative darkfield intensity values to darkfield-to-total ratios.

F.D. Ingram: Could the continuum signal that you monitor routinely for elemental concentration determination using the p/b method be ratioed with the film continuum and calibrated to provide sample dry solids content in a manner similar to that described using the scattered beam? There might be advantages to using the continuum signal instead of the scattered beam for this purpose. It makes use of available data, and because it does not require an independent measurement, it might be simpler and more straightforward to interpret. The argument has been presented that the continuum determination is inaccurate because of scattered beam, etc. If it is not sufficiently accurate for total solids determination, how can its use be justified for elemental concentration measurement?

Author: I agree with your arguments to measure the dry mass portion by the X-ray continuum signal. Unfortunately, experiments to estimate the local dry weight content in freeze-dried cryosections from X-ray continuum measurements resulted in too large scattering of data. The correct determination of the extraneous background turned out to be very critical. The peak-to-back-

ground ratio, however, was found to be much less sensitive for errors in the continuum measurements. Perhaps your suggestion will be realized in the future by an improved evaluation program.

R. Reichelt: The precise quantification of the concentration of an element X requires an exact knowledge about the fractions f+e of the continuum radiation in equation (1). Is there a certain proof that the fraction f+e does not depend on the specimen and its scattering properties, respectively?

Author: Basically, the fraction f+e depends also on the specimen. However, the influence of an ultrathin section composed only of low atomic number elements should be extremely small in comparison with the total amount of e+f, measured in the absence of any specimen.

F.D. Ingram: Mass loss is a fact of life in electron microscopy. The nature of loss and rate of loss appear to be altered by use of a cold stage, but there is no agreement that it is entirely eliminated. Is it not necessary that you establish that each measurement is sufficiently free of mass loss to permit interpretation of data in terms of tissue solids content and hence water content?

Author: Of course one prerequisite of quantitative X-ray microanalysis is that the specimen does not change during the measurement. Neither mass loss nor contamination is observed in completely freeze-dried sections, studied in the cold stage of the STEM at 138 K. However, even small amounts of water remaining in the section induce remarkable mass loss, which affects the quantitative evaluation of the obtained data.